

Experimental Comparison of Human Gait Tracking Algorithms: Towards a Context-Aware Mobility Assistance Robotic Walker

Georgia Chalvatzaki¹, Xanthi S. Papageorgiou¹, Christian Werner²,
Klaus Hauer², Costas S. Tzafestas¹ and Petros Maragos¹

¹ School of Electrical and Computer Engineering, National Technical University of Athens, Greece

² Agaplesion, Bethanien Hospital - Geriatric Centre at the University of Heidelberg, Germany

{gchal, xpapag}@mail.ntua.gr, {Christian.Werner, khauer}@bethanien-heidelberg.de,

{ktzaf, maragos}@cs.ntua.gr

Abstract—Towards a mobility assistance robot for the elderly, it is essential to develop a robust and accurate gait tracking system. Various pathologies cause mobility inabilities to the aged population, leading to different gait patterns and walking speed. In this work, we present the experimental comparison of two user leg tracking systems of a robotic assistance walker, using data collected by a laser range sensor. The first one is a Kalman Filter tracking system, while the second one proposes the use of Particle Filters. The tracking systems provide the positions and velocities of the user’s legs, which are used as observations into an HMM-based gait phases recognition system. The spatiotemporal results of the HMM framework are employed for computing parameters that characterize the human motion, which subsequently can be used to assess and distinguish between possible motion disabilities. For the experimental comparison, we are using real data collected from an ensemble of different elderly persons with a number of pathologies, and ground truth data from a GaitRite System. The results presented in this work, demonstrate the applicability of the tracking systems in real test cases.

I. INTRODUCTION

A. Motivation

Mobility problems are common in the elderly, as they have to cope with instability and lower walking speed, [1]. Certain pathologies are responsible for changes in stride length and in walking phases, [2]. Elder care constitutes a major issue for modern societies, and the use of non-invasive methods for medical monitoring is crucial. Robotics seems to fit naturally to the role of assistance, since it can incorporate features such as posture support and stability, walking assistance, health monitoring, etc.

Our aim is to use intelligent robotic platforms (Fig.1), which can monitor and understand the patient’s walking state and will autonomously reason on performing assistive actions regarding the patient’s mobility and ambulation, [3]. We are working on the development of an Adaptive Context-Aware Robot Control architecture, when the robotic assistant is in front of the user and detects the patient’s mobility state by using real-time laser data. We recognize specific gait patterns and also compute gait parameters that are indicative of particular pathologies, [4]. This indication will trigger

This research work was supported by the European Union under the project “MOBOT” with grant FP7-ICT-2011-9 2.1 - 600796.

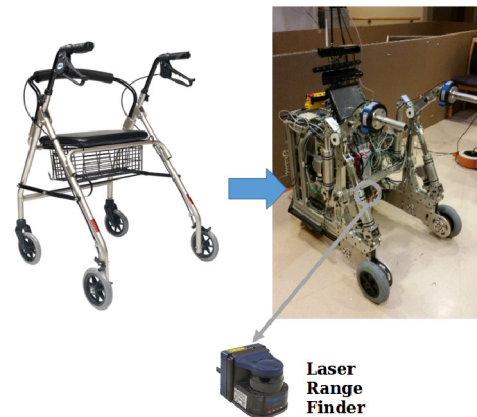


Fig. 1: Left: Typical market-based passive assistive device for elderly. Right: A robotic platform, constructed with financial support of EU project MOBOT, equipped with a Hokuyo Laser Sensor aiming to record the experimental gait data of the user (below knee level).

control assistive actions and behaviors (velocity adjustment, approach of the patient due to changes in gait patterns) from the robotic assistant that follows the user. It is therefore crucial to have a robust tracking system, as the estimated gait parameters of the user are essential for the low level robot controller, [5].

In this paper, we address the challenge of developing a reliable pathological gait tracking system. The proposed system utilizes a laser sensor that detects the user (which does not interfere with human motion). We test two different leg tracking approaches, for extracting the necessary gait parameters. The first approach is based on K-means clustering and Kalman Filtering. The second approach is based on Particle Filter, which tracks each leg separately, while performing a data association for the two targets-legs. The results of both methods, i.e. the estimated leg positions and velocities are the observations of a Hidden Markov Model (HMM) for recognizing the different gait phases. This information is then used to extract the gait parameters. Our goal is to employ this setup as a subsystem within a larger behaviour-based robot control framework for the development of a cognitive context-aware walking-aid robot.

B. Related Work

The automatic classification and modeling of specific human activities is useful for many technical and biomechanical applications. A number of research groups worldwide, are actively pursuing research, investigating problems related to the development of smart walking support devices, aiming to assist motor-impaired persons and elderly in standing, walking and other mobility activities, as well as to detect abnormalities and to assess rehabilitation procedures, [6], [7]. Many researchers cope with gait analysis using machine learning algorithms, aiming to detect pathological cases that require medical treatment, using sparse representation for the detection of Parkinsonian gait patterns, [8].

For extracting gait motions, different types of sensors have been used, from gyroscopes and accelerometers to cameras, e.g. [9], [10]. Other approaches refer to human detection and tracking, or recognition of human activity utilizing laser sensors, and in some cases complementary with cameras, or force sensors, [11]. The detection and tracking of humans is a common problem. Most research work focuses on detecting and tracking human legs from static sensors, as in pedestrian tracking, [12], or from laser scanners mounted on mobile robotic platforms for person following, [13], [14]. Approaches for tracking users of robotic walkers can be found in [15], [16]. Human tracking with particle filters using laser scanners mounted on mobile robots can be found in [17], [18], while in [19] the researchers used two laser scanners and a particle filter-based prediction of the legs' positions and velocities used as input to a PID controller for the mobile robot. Several works use the GAITRite System for validating their gait analysis results, [20]. GAITRite System is commonly used for gait impairments detection and analysis, [21].

Gait analysis can be achieved by using Hidden Markov Models (HMMs), which can model the dynamic properties of walking. The versatility of HMMs makes them useful in extracting human patterns. HMMs are currently used for gait modelling employing data from wearable sensors, like gyroscopes mounted on human's feet, [22].

This paper presents a comparative study of two tracking frameworks, the first is based on Kalman Filter and the second one uses Particle Filters with a data association technique, that were developed for the estimation of the legs' positions and velocities of a subject using a robotic assistant platform (Fig. 1). The estimated parameters are fed into an HMM-based gait recognition system, that detects specific phases of human walking. Given that segmentation we can extract spatiotemporal gait parameters, which will be used for the impairment level assessment of the user in an Adaptive Context-Aware Robot Control architecture. Instead of using complex models and motion tracking approaches that require expensive or bulky sensors and recording devices that interrupt human motion, the measured data used in this work are provided by a standard laser rangefinder sensor mounted on a robotic rollator platform. In this work, we aim to compare the performance of the two tracking methods

by testing their accuracy in extracting gait parameters with respect to the ground truth data from a GAITRite System and their robustness in tracking the user in difficult cases, such as occlusions or cluttered environment.

II. HUMAN GAIT CYCLE ANALYSIS

The human gait motion analysis is based on the periodic movement of each foot from one position of support to the next, [23]. The gait cycle is divided into eight events. This segmentation is sufficiently general to be applied to most types of human gait, including five during stance phase (the foot is on the ground) and three during swing (the same foot is no longer in contact with the ground), [24]. The internal gait phases are (as a percentage of the total duration of the gait cycle): 1. **IC** - Initial Contact: 0%, 2. **LR** - Loading Response: 0-10%, 3. **MS** - Midstance: 10-30%, 4. **TS** - Terminal Stance: 30-50%, 5. **PW** - Preswing: 50-60%, 6. **IW** - Initial Swing: 60-70%, 7. **MW** - Midswing: 70-85%, 8. **TW** - Terminal Swing: 85-100%. In this paper, we have used the seven gait phases of walking in order to analyze the gait cycle, since the TW phase is an equivalent trigger to the IC phase, and therefore are treated as identical.

Specific gait parameters can be computed at every walking cycle, which are commonly used for medical diagnosis, [4], [25]. In this work, we are using three temporal parameters: 1) **stride time**: the duration of each gait cycle, 2) **swing time**: the swing phase duration in a gait cycle, 3) **stance time**: the stance phase duration in one cycle, and three spatial parameters: 1) **stride length**, i.e. the distance traveled by both feet in a gait cycle, 2) **right step length**: the mean distance traveled by the right leg and 3) **left step length**: the mean distance traveled by the left leg in a gait cycle.

III. GAIT PARAMETERS EXTRACTION BASED ON HIDDEN MARKOV MODEL

Hidden Markov Models are well suited for gait recognition due to their statistical properties and their ability to reflect the temporal state-transition nature of gait. In our previous work, we analyze extensively the properties of our HMM system and its applications for modelling normal human gait, [26], as well as for pathological gait recognition, [27].

A. HMM Gait Cycle Recognition

The seven gait phases can define the hidden states of the HMM. As observables, we utilize several quantities that represent the motion of the subjects' legs, (relative position w.r.t. the laser, velocities, etc.), which are estimated using sequential signals from a laser sensor. We consider seven hidden states according to the seven gait phases, while the observations are the legs' positions and velocities along the axes and the the distance between the legs. The observation data are modeled using a mixture of Gaussian distributions (GMM). The observations at each time instant are expected to be extracted by the raw laser data collected by the laser range scanner mounted on the robotic rollator (the measurements are relative to the robotic platform motion), Fig. 1. We will, later, discuss the implementation of two

different approaches for the estimation of the user's legs kinematic parameters, that are used as observables for the HMM framework.

B. Gait Parameters Extraction

The recognized sequence of gait phases is indicative of the subject's underlying pathology, since it differs from the normal gait phase sequences. Using this segmentation we can compute the gait parameters from the range data. Each recognized gait cycle is used for the gait parameter extraction. The *stride time* equals the duration of the recognized gait cycle. Given the time segmentation by the HMM, we have isolated the stance and swing phase of the gait cycle, and computed the *swing time* between the gait phases **IW** and **MW** and the stance time between the gait phases **IC** and **PW**. The *right and left step lengths* are computed by the absolute maximum distance traveled by each leg, while their summation during the gait cycle provides the *stride length*.

IV. TRACKING USER'S LEGS USING KALMAN FILTERING

This detection and tracking system of the subject's legs uses K-means clustering and Kalman Filtering (**KF**) for the estimation of the central positions and velocities of the left and right leg along the axes, [27]. Towards detecting the user's legs we preprocess the raw laser data at each time frame. A rectangle observation window is defined in the walking plane, which is wide enough for initialization, while in the consecutive frames it is adjusted according to the uncertainty of the predicted legs' positions. The laser points lying outside the window are discarded, while the remaining are separated into groups according to a euclidean distance threshold between consecutive laser points. The laser groups containing less points than a pre-specified number are deleted. We wish to end up with two groups (handling of cases with more than two groups are discussed later), which are labeled as left/right leg by the K-means clustering algorithm. Circle Fitting is used for computing the legs' centers, which compose the observation vector, z_k , for the tracking process.

The state vector of the user's legs used in KF comprises the state vectors of both legs: $x_k^{left} = [x^L \ y^L \ v_x^L \ v_y^L]^T$ and $x_k^{right} = [x^R \ y^R \ v_x^R \ v_y^R]^T$, where (x^L, y^L) and (x^R, y^R) are the Cartesian coordinates of the centroid legs' positions w.r.t laser, and (v_x^L, v_y^L) , (v_x^R, v_y^R) are their velocities along the axes, at time instant k . Thus, the KF state vector is: $x_k = \begin{bmatrix} (x_k^{left})^T & (x_k^{right})^T \end{bmatrix}^T$. We use the standard KF state equations: $x_k = A_k x_{k-1} + B_k u_{k-1} + w_k$, where k refers to time, x_k is the state vector, u_k is the input vector, A_k is the state transition matrix, B_k is the input matrix and w_k is the process noise with normal probability distribution $p(w_k) \sim N(0, Q_k)$, where Q_k is the process noise covariance matrix. The observation vector z_k of the true state is updated according to the standard equation: $z_k = H_k x_k + v_k$, where H_k is the observation matrix, which maps the true state space into the observed space, and v_k is the observation noise, following the normal distribution $p(v_k) \sim N(0, R_k)$, where R_k

is the measurement noise covariance matrix. Since we have no direct influence on the acceleration (it is "user" generated) nor any measurements, we treat it as the process noise.

The predictions of the KF are used as seed for the K-means algorithm. Around the legs' predicted positions we place the observation window, which is adaptively adjusted according to the KF prediction variability. The detected raw data inside it, are ready to be preprocessed. Thus, the described method results in an iterative interaction between detection and tracking processes. The predicted positions are fed back to the preprocessing stage as a prior information of the expected positions of the legs for the next time frame.

If one leg is occluded by the other (common problem while turning) or there is interference of the carer's legs (clutter), we have a false detection case. A false detection occurs during leg detection process, whenever more than two groups of laser points appear or there is a violation of a distance threshold from the detected legs' centers. Then, we do not account any observations, but we only apply the prediction step of the KF. However, if we cannot track the user for over 5 time frames we re-initialize the system.

V. TRACKING USER'S LEGS USING PARTICLE FILTERING WITH DATA ASSOCIATION

We have designed a Particle Filter (**PF**) Leg Tracker to deal with problems in the performance of the KF tracking, such as tracking loss in cases of long time occlusions. We have used the particle filter theory, [28], for tracking each leg separately and applied a probabilistical data association, [29], of the legs.

We use two particle filters to estimate the posteriors of the legs' states x_k^{left} and x_k^{right} at each time instant k . The particles represent samples of the posterior density distribution of the legs' states. At the first time instant $k=1$, we initialize the particles of each leg by drawing N samples from an initial prior distribution.

For approximating the true posterior of the state we have used the Sequential Importance Resampling method (SIR PF), [28]. According to SIR PF, every new time frame $k=2, \dots, T$, (where T is the total tracking time), the new particles of the state are sampled from the importance density function: $x_k^{f,i} \sim p(x_k^f | x_{k-1}^f)$, where $f = \{left, right\}$ and i denotes the i^{th} sample. This distribution function represents the transition probability of the state from time $k-1$ to time k and constitutes the motion model, that propagates the particles' state of each leg at each time instant k , given the previously estimated state x_{k-1}^f . We considered the fact that the leg motion does not follow a constant velocity or acceleration model, but have variable velocity according to its gait phase. We model the velocity of each leg along the axes by a GMM of two mixtures. Every time instant k , we draw N velocity samples for each leg. Those samples are then used for updating the particles position through time, by adding to the previous estimated leg position the displacement imposed by the new velocity of each particle along the axes.

After the particles are propagated through time, we need to associate each particle set with the corresponding laser points of the left/right leg. Inspired by the methodology in data association literature, [30], we take as observations only the laser points that fall inside a particle gate. In this work, a particle gate is an experimentally defined rectangular area centered around each particle, so that every sample $x_k^{f,i}$ refers to a different cluster of laser points, $y_k^{f,i}$. Because we have defined the prior distribution to be equal to the proposal distribution, the particle weights are equal to the observation likelihood: $\omega_k^{f,i} = p(y_k^{f,i}|x_k^{f,i})$. Considering the circular representation of the legs described in Section IV, the observation likelihood evaluates how the laser points are distributed on the circular contour given the center, which is the particle's position for each leg. Thus, we have divided horizontally the circle into two semicircles. Laser points in the upper semicircle do not contribute to the observation likelihood. The lower semicircle is split into M regions R_l with $l = 1, \dots, M$, of equal angle range and we have evaluated the normal distribution of the distances of the laser points of each region with respect to the corresponding particle position, which is a candidate leg center.

Because the human legs are two interacting moving targets, we introduce an association probability β_i , that regulates the observation likelihood of the one leg with respect to the other, by evaluating a likelihood of the Euclidean distance of the two legs modeled by a Gamma distribution. Finally, the observation likelihood for each leg is computed using the following function: $p(y_k^{f,i}|x_k^{f,i}) = \beta_i \cdot \left[\lambda_i \cdot \sum_{l=1}^4 \pi_l \cdot \prod_{j \in R_l} \mathcal{N}(d_j|\mu_l, \Sigma_l) \right]$ where $y_k^{f,i} = [(x_j, y_j)]$, is the set of the laser points in the gate of the i^{th} particle of each leg, $j \in R_l$, where R_l is the l^{th} region of laser points, $\mathcal{N}(d_j|\mu_l, \Sigma_l)$ is the normal distribution of the distances d_j of the laser points of each region from the i^{th} particle, μ_l is the mean vector and Σ_l is the covariance matrix of the normal distribution for each region R_l . The π_l are the importance weights of the regions, which were set so that the extreme regions, which often contain many outliers, have less importance; λ_i is a scaling factor that depends on the cluster length for the i^{th} particle. All parameters have been experimentally defined. The weights are normalized according to: $\hat{\omega}_k^{f,i} = \omega_k^{f,i} / \sum_{j=1}^N \omega_k^{f,j}$. To overcome weight degeneracy, i.e. when most particles have infinitely small weight, we use the systematic resampling method, [28], [31], for eliminating particles with small weights and replicating particles with higher weights. Finally, the state's posterior estimate is approximated by the Minimum Mean Square Error (MMSE): $x_k^f = \sum_{i=1}^N \hat{\omega}_k^{f,i} x_k^{f,i}$.

VI. EXPERIMENTAL ANALYSIS & VALIDATION

A. Experimental setup and data description

The experimental data used in this work were collected in Agaplesion Bethanien Hospital - Geriatric Center. Patients

with moderate to mild impairment, according to clinical evaluation of the medical associates, took part in this experiment. The patients were wearing their normal clothes (no need for specific clothing nor there was placement of visual markers on them). We have used a Hokuyo rapid laser sensor (UBG-04LX-F01 with mean sampling period of about 28msec), mounted on the robotic platform of Fig. 1 for the detection of the patients' legs. A GAITRite System was used to collect ground truth data. GAITRite is an electronic mat, equipped with pressure sensors placed at 1.27 cm each, used for gait analysis. GAITRite provides measurements of the spatial and temporal gait parameters and is commonly used for medical diagnosis, [20].

We have used data from four patients with moderate mobility impairment (aged over 65 years old). Each subject walked straight with physical support of the robotic rollator over the walkway defined by the GAITRite mat. All patients performed the experimental scenarios under appropriate carer's supervision. The subjects were instructed to walk as normally as possible. This results in a different walking speed for each subject, and in different gait parameters.

In Fig. 2, snapshots of a subject are presented, while performing the experimental scenario, captured by the Kinect camera that was also mounted on the robotic rollator (Fig. 1). Also, in Fig. 3 the sequence of the detected footprints by the GAITRite System for the same subject are depicted.

B. Validation Strategy

In this work the comparison of the KF-based tracking system and the PF leg tracker is presented. The latter was tested with 300 particles per leg for a correct tracking, which is less than the respective amount of samples used by other researches that used data from a laser scanner to track humans, [17]–[19]. We will use the gait parameters measured by the GAITRite System as ground truth data to validate the results. We ascertain if the tracking results of the two filters alters the gait phase recognition by the HMM-based methodology and if so, to check which filter combined with HMM produces gait parameters that converge better to the ground truth data.

We have isolated the laser data corresponding to the respective strides detected on the GAITRite mat. These data were processed according to the two approaches, in order to extract the gait parameters, as described in subsection III-B. The HMM training procedure comprises estimation data from the KF tracking system for 12 different patients that performed the experimental scenario without the GaitRite mat. The evaluation is based on an assessment of the estimated states provided by the constructed HMM, which represents the human gait cycle. Data from all patients that performed the experimental scenario on the GAITRite mat are used for testing.

The validation of the results comprises both quantitative and qualitative comparisons. Table I contains the mean and standard deviations of the gait parameters, as those were estimated using as input to the HMM recognition system the observations by the two methods, in order to compare the

TABLE I: Extracted Gait Parameters

Subject	Parameter	Unit	HMM-KF	HMM-PF	GAITRite
1	stride length	m	0.73 ± 0.05	0.71 ± 0.01	0.75 ± 0.01
	right step	m	0.36 ± 0.02	0.35 ± 0.01	0.39 ± 0.04
	left step	m	0.37 ± 0.04	0.36 ± 0.05	0.36 ± 0.01
	stride time	s	1.11 ± 0.09	1.06 ± 0.02	1.10 ± 0.02
	swing time	s	0.37 ± 0.04	0.38 ± 0.05	0.41 ± 0.02
	stance time	s	0.73 ± 0.05	0.68 ± 0.04	0.61 ± 0.04
2	stride length	m	0.93 ± 0.02	0.88 ± 0.05	0.86 ± 0.05
	right step	m	0.44 ± 0.07	0.43 ± 0.03	0.44 ± 0.02
	left step	m	0.46 ± 0.02	0.45 ± 0.02	0.42 ± 0.04
	stride time	s	1.03 ± 0.03	1.03 ± 0.03	1.07 ± 0.05
	swing time	s	0.32 ± 0.01	0.34 ± 0.06	0.44 ± 0.01
	stance time	s	0.72 ± 0.03	0.69 ± 0.08	0.60 ± 0.09
3	stride length	m	0.57 ± 0.06	0.57 ± 0.04	0.57 ± 0.03
	right step	m	0.27 ± 0.01	0.26 ± 0.02	0.26 ± 0.03
	left step	m	0.30 ± 0.01	0.31 ± 0.03	0.31 ± 0.01
	stride time	s	1.17 ± 0.04	1.18 ± 0.05	1.19 ± 0.03
	swing time	s	0.32 ± 0.02	0.34 ± 0.06	0.47 ± 0.04
	stance time	s	0.84 ± 0.03	0.84 ± 0.04	0.73 ± 0.03
4	stride length	m	0.71 ± 0.08	0.68 ± 0.03	0.68 ± 0.03
	right step	m	0.35 ± 0.01	0.34 ± 0.07	0.34 ± 0.02
	left step	m	0.36 ± 0.01	0.34 ± 0.03	0.34 ± 0.01
	stride time	s	1.18 ± 0.06	1.21 ± 0.07	1.19 ± 0.03
	swing time	s	0.37 ± 0.06	0.32 ± 0.09	0.44 ± 0.04
	stance time	s	0.81 ± 0.01	0.89 ± 0.01	0.73 ± 0.07

Gait parameters means and standard deviations computed by the HMM recognition system using as observations the KF and PF estimates, along with the ground truth measured parameters of the GAITRite System for the four subjects.

TABLE II: Accuracy measures

	MEAN		RMSE		MAD	
	KF	PF	KF	PF	KF	PF
stride length (m)	0.063	-0.013	0.043	0.036	0.030	0.023
right step (m)	-0.008	-0.010	0.031	0.042	0.024	0.028
left step (m)	0.060	-0.016	0.046	0.026	0.033	0.034
stride time (s)	-0.019	-0.024	0.066	0.051	0.047	0.035
swing time (s)	-0.101	-0.093	0.116	0.116	0.042	0.060
stance time (s)	0.079	0.057	0.091	0.085	0.035	0.057

Statistical comparison of the two filters using the measures Mean error, rms error (RMSE) and mean absolute deviation (MAD) error of the estimated gait parameters from the ground truth data.

TABLE III: Tracking Robustness

Subject		Total Tracking time (s)	Total errors (# frames)	Total errors (% of total frames)
1	KF	16.97	1	0.16
	PF	17.00	0	0
2	KF	13.10	64	12
	PF	14.89	0	0
3	KF	13.52	47	8.89
	PF	14.84	0	0
4	KF	13.05	7	1.48
	PF	13.24	0	0

Total tracking time and tracking errors for all subjects for evaluating the tracking robustness of the two filters.

accuracy of the tracking systems. Table II presents the Mean error, the Root Mean square Error (RMSE) and the Median Absolute Deviation (MAD) of the errors of the estimated gait parameters from the KF-HMM and the PF-HMM systems from the GAITRite ground truth data.

Furthermore, we present results of laser frames where we can inspect the actual performance of the two systems in cases of occlusions, etc., and we compute the parameters total tracking errors and total time of tracking, presented in Table III, in order to account for the tracking robustness of the two implementations.

C. Validation Results and Discussion

1) *Accuracy*: Inspecting the results of Table I, it is obvious that both filters converge quite well to the ground truth data. Table II contains the statistics for the errors of the filters from the ground truth data. We can see that the spatial parameters errors for both filters are quite small. We should consider that the GAITRite system refers to the foot impact for measuring the gait parameters, while our raw data are provided by a laser range scanner that detects the human tibia, so they depend on the subject's height, and also the movement of the lower limb, while the motion of its hypothetical center, is not aligned with the heel center movement, making the extraction of the gait parameters even more difficult. However, in most cases the PF tracking system performs better than the KF. As for the temporal parameters, we detect larger errors in the swing/stance time segmentation for both filters, but the results clearly demonstrate that there is significant space for increasing the accuracy of the HMM-based recognition system.

2) *Robustness*: In Fig. 4 we present results that would help us evaluate the tracking robustness of the two filters. In Fig 4a, 4c the black stars represent the raw laser data, the red 'x' the left estimated and the green 'x' the left detected leg position, while the blue 'x' is the right estimated and the magenta 'x' the right detected leg position. In Fig. 4b, 4d the black stars represent the raw laser data. The green circles are the left leg particles and the red 'x' is the position estimate, while the magenta circles are the right leg particles and the blue 'x' is the estimation. Fig. 4a, 4b show a typical case of cluttered environment, for which the KF wrongly estimates the position of the two legs while the PF performs well. In Fig. 4c, 4d we present a case of leg occlusion, where once more the PF predicts the occluded left leg's position, while the KF detection and tracking strategy fails to predict correctly the position of both legs. Also, the proposed computation of the observation likelihood for the PF tracker with the data association gives better results than the KF tracker, in cases of great noise, e.g due to clothing, where the KF tracking system fails most of the times to correctly estimate the leg centers, while the PF observation likelihood penalizes points that seem to be outliers.

Table III presents the total time of correct tracking, the total tracking errors in frames and the total errors as a percentage of the total frames provided by the laser scanner. The PF tracks all the users successfully, while the KF tracking system loses track of the user many times, especially subjects #2 and #3, who presented different types of walking according to Table I, i.e. subject #2 did larger strides than subject #3. This is also an indication of the applicability of the two filters regarding large variations on gait speed, that cannot be successfully modeled by the linear motion model of the KF tracking system.

VII. CONCLUSIONS AND FUTURE WORK

We aim to develop a completely non-invasive pathological walking analysis and assessment system, as a subsystem of a context-aware robot control for an intelligent robotic



Fig. 2: Snapshots of a subject walking on the GAITRite walkway assisted by the robotic platform, during one stride.



Fig. 3: The captured footprints of the subject by the GAITRite System.

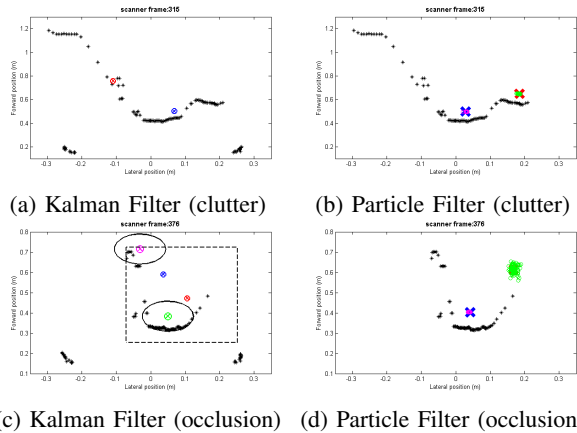


Fig. 4: Snapshots of false detection from Kalman Filter that can be handled well by Particle filter. (a) KF estimated leg positions in clutter, (b) PF estimation in clutter. (c) KF estimation while left leg is occluded and (d) PF estimation during left leg occlusion.

walker. An accurate and robust tracking system of the user's legs is a crucial parameter for the control system. Thus, we compare a tracking system based on K-means clustering and Kalman Filter, with a Particle Filters leg tracking framework. A typical laser rangefinder sensor provides data, constituting a non-invasive approach using a non-wearable device. The two methodologies are compared using ground truth data from a GAITRite System, and both can successfully extract the gait parameters in most cases. The experimental results clearly show that the PF tracker is more reliable than the KF tracking system, as it is more accurate in estimating the gait parameters and it can also successfully handle difficult cases, such as leg occlusions and environmental clutter. But there is still room for further accuracy increase on the PF tracking system and the HMM-based gait recognition framework.

Our goal is to implement a multilayered particle filter tracking system, that will incorporate multiple modalities such as visual cues, for an augmented state estimation of the user. We aim to increase the filter accuracy by testing particle filter smoothing techniques and by using multiple motion models according to the patient's impairment level, that will populate the samples of the particle filter leg tracker according to the patient's walking speed. We intend to create a system for detecting in real time specific gait pathologies and automatically classify the patient status or the rehabilitation progress, thus providing the necessary information for effective cognitive active mobility assistance robots.

REFERENCES

- [1] T. Herman et. al, "Gait instability and fractal dynamics of older adults with a cautious gait: why do certain older adults walk fearfully?" *Gait Posture* 2005.
- [2] J. M. Hausdorff, "Gait dynamics, fractals and falls: Finding meaning in the stride-to-stride fluctuations of human walking," *Human Movement Science* 2007.
- [3] X. Papageorgiou et. al., "Advances in intelligent mobility assistance robot integrating multimodal sensory processing," *Lecture Notes in Computer Science, Universal Access in Human-Computer Interaction. Aging and Assistive Environments*, 2014.
- [4] A. Muro-de-la-Herran et. al., "Gait analysis methods: An overview of wearable and non-wearable systems, highlighting clinical applications," *Sensors* 2014.
- [5] G. Chalvatzaki et. al, "Gait modelling for a context-aware user-adaptive robotic assistant platform," in *IMAACA* 2015.
- [6] M. Spenko et. al., "Robotic personal aids for mobility and monitoring for the elderly," *IEEE Trans. on Neural Systems and Rehabilitation Engineering*, 2006.
- [7] J. Lin et. al., "Automatic human motion segmentation and identification using feature guided hmm for physical rehabilitation exercises," in *IROS*, 2011.
- [8] Y. Zhang et. al., "Pathological gait detection of parkinson's disease using sparse representation," in *DICTA*, 2013.
- [9] J. Bae and M. Tomizuka, "Gait phase analysis based on a hidden markov model," *Mechatronics*, 2011.
- [10] C. Nickel et. al., "Using hidden markov models for accelerometer-based biometric gait recognition," in *CSPA* 2011.
- [11] A. Panangadan et. al., "Tracking and modeling of human activity using laser rangefinders," *Int'l Journal of Social Robotics*, 2010.
- [12] X. Shao et. al., "Analyzing pedestrians' walking patterns using single-row laser range scanners," in *ISIC*, 2006.
- [13] T. Horiuchi et. al., "Pedestrian tracking from a mobile robot using a laser range finder," in *ISIC* 2007.
- [14] K. Arras et. al., "Efficient people tracking in laser range data using a multi-hypothesis leg-tracker with adaptive occlusion probabilities." *ICRA*, 2008.
- [15] H. Kim et. al., "Detection and tracking of human legs for a mobile service robot," in *AIM* 2010.
- [16] W.-H. Mou et. al., "Context-aware assisted interactive robotic walker for parkinson's disease patients," in *IROS* 2012.
- [17] N. Belloto and H. Hu, "People tracking with a mobile robot: A comparison of kalman and particle filters." *IATED* 2007.
- [18] P. Chakravarty et. al., "Panoramic vision and laser range finder fusion for multiple person tracking," in *IROS* 2006.
- [19] T. Ohnuma et. al., "Particle filter based lower limb prediction and motion control for jaist active robotic walker," in *2014 RO-MAN*.
- [20] A. Rampp et. al., "Inertial sensor-based stride parameter calculation from gait sequences in geriatric patients," *IEEE Trans. Biomed. Engineering*, 2015.
- [21] U. Givon et. al., "Gait analysis in multiple sclerosis: Characterization of temporalspatial parameters using {GAITRite} functional ambulation system," *Gait Posture* 2009.
- [22] A. Mannini et. al., "Online decoding of hidden markov models for gait event detection using foot-mounted gyroscopes," *IEEE JBHI*, 2014.
- [23] H. Inman et. al., "Human walking". Williams & Wilkins, 1981.
- [24] J. Perry, "Gait Analysis: Normal and Pathological Function", 1992.
- [25] R. Kressig et. al., "Temporal and spatial features of gait in older adults transitioning to frailty," *Gait Posture* 2004.
- [26] X. Papageorgiou et. al., "Hidden markov modeling of human normal gait using laser range finder for a mobility assistance robot," in *ICRA* 2014.
- [27] —, "Hidden markov modeling of human pathological gait using laser range finder for an assisted living intelligent robotic walker," in *IROS* 2015.
- [28] M. Arulampalam et. al., "A tutorial on particle filters for online nonlinear/non-gaussian bayesian tracking," *IEEE Trans. Signal Processing*, 2002.
- [29] D. Schulz et. al., "People tracking with a mobile robot using sample-based joint probabilistic data association filters," *Int. J. Robot. Res.* 2003.
- [30] A. Tchango et. al., "Tracking multiple interacting targets using a joint probabilistic data association filter," in *FUSION* 2014.
- [31] M. Bolić et. al., "Resampling algorithms for particle filters: A computational complexity perspective," *EURASIP* 2014.